Prospects for discovering strongly decaying doubly heavy T_{bc} tetraquark states at LHCb*

Mingjie Feng (冯铭婕)[1,2] Yiming Li (李一鸣)[1†] Hua-Sheng Shao (邵华圣)[3]

[1]Institute of High Energy Physics, Chinese Academy of Science, Beijing 100049, China
[2]University of Chinese Academy of Science, Beijing 100049, China
[3]Laboratoire de Physique Théorique et Hautes Energies (LPTHE), UMR 7589, Sorbonne Université et CNRS, 4 place Jussieu, 75252 Paris, France

Abstract: We investigate the discovery potential of the T_{bc} state with $J^P = 0^+$ in proton-proton (pp) collisions at LHCb at a center-of-mass energy of $\sqrt{s} = 13$ TeV. The study focuses on the decay channel $T_{bc} \to B^- D^+$. A phenomenological approach is employed to construct the background model based on the associated production of B and D mesons, incorporating previously published LHCb results. Background processes are simulated using `MadGraph5_aMC@NLO` and `Pythia8.3`. We explore the parameter space of the T_{bc} mass, width, production cross section, and the effective double-parton scattering cross section ($\sigma_{\rm eff}$) relevant for the BD meson background. The integrated luminosity required for a 5σ discovery at LHCb is evaluated under various assumptions. In particular, we consider three representative T_{bc} production cross section scenarios: an optimistic estimate of 103 nb, an intermediate value of 18 nb obtained by scaling from the T_{cc}^+ production cross section, and a conservative lower bound of 0.3 nb. We find that a 5σ observation is achievable for a production cross section of 103 nb, which is expected to be within reach during Run~4. In contrast, the more realistic cross section estimate of 18 nb requires the full Run~5 dataset (300 fb^{-1}) under the most favorable parameter choices. For the conservative scenario, no significant signal would be observable even with 300 fb^{-1}. In addition, we estimate the minimum observable $\sigma(T_{bc}) \times \mathcal{B}(T_{bc} \to B^- D^+)$ for a 5σ discovery under different luminosity scenarios, providing guidance for future experimental searches at LHCb.

Keywords: doubly heavy tetraquarks, associated production, LHCb experiment

DOI: 10.1088/1674-1137/ae5a87 **CSTR:**

I. INTRODUCTION

Since the discovery of the $X(3872)$ by the Belle experiment in 2003 [1], numerous resonant states have been observed that lie beyond the conventional quark-model description of the hadron spectrum. These observations have significantly broadened our understanding of hadron spectroscopy. Exotic hadrons also play an important role in the study of quantum chromodynamics (QCD), as they provide a unique window into the non-perturbative dynamics of the strong interaction. Consequently, the investigation of exotic hadronic states has become a frontier of hadron physics over the past two decades. A wide variety of theoretical models have been proposed, accompanied by extensive experimental efforts to search for new exotic states via various production mechanisms and to measure their masses, widths, production cross sections, and spin-parity quantum numbers to elucidate their internal structure.

The observation of the doubly charmed tetraquark T_{cc}^+ and the doubly charmed baryon Ξ_{cc}^{++} in proton–proton collisions [2, 3] has firmly established that hadrons containing two heavy quarks can be produced promptly at hadron colliders. These discoveries open a new frontier in the search for other doubly heavy systems, among which the T_{bc} and T_{bb} tetraquarks have yet to be observed experimentally.

Unlike the doubly charmed case, the T_{bc} contains two different heavy flavors, namely a bottom quark and a charm quark. This distinctive composition makes it an invaluable probe of non-perturbative QCD dynamics in sys-

Received 19 January 2026; Accepted 1 April 2026

* The work of MF and YL is supported by the National Natural Science Foundation of China (NSFC) (grant No.12175245, 12188102, W2443008). The work of HSS is supported by the European Research Council (grant No.101041109, "BOSON") and the French National Research Agency (grant ANR-20-CE31-0015, "PrecisOnium")

† E-mail: liyiming@ihep.ac.cn

tems with unequal heavy-quark masses. It provides a unique opportunity to test heavy-quark symmetry and its breaking, explore the flavor dependence of diquark correlations, and constrain models of multiquark binding [4, 5]. Its discovery would enrich the spectrum of doubly heavy tetraquarks and deepen our understanding of exotic hadron structure.

Numerous theoretical predictions exist for the ground-state mass of the $T_{bc}(bc\bar{u}\bar{d})$ tetraquark (charge conjugation is implied throughout this paper). The T_{bc} mass is generally expected to lie close to the open-bottom–open-charm meson threshold. The predicted mass difference with respect to the $\bar{B}D$ threshold falls in the range [5−14]

$$-50\ \text{MeV} < m(T_{bc}) - m(\bar{B}) - m(D) < 120\ \text{MeV}. \quad (1)$$

At present, it remains unclear whether the T_{bc} mass lies above or below the $\bar{B}D$ threshold. If the mass lies below threshold, the T_{bc} would be stable against strong decays and could only be accessed via weak interactions [6−11]. Detailed studies of the weak decay modes of such a doubly heavy tetraquark, including both semileptonic and nonleptonic channels induced by b- or c-quark decays, have been performed using flavor SU(3) symmetry in ref. [15]. It is worth noting that weak decay channels may also provide promising discovery opportunities for T_{bc} states at LHCb, and related experimental studies are ongoing. If the mass lies above threshold, the T_{bc} is expected to appear as a relatively narrow resonance in the $\bar{B}D$ invariant-mass spectrum and can therefore be searched for directly [5, 12−14]. In this study, we focus on the latter scenario, where the T_{bc} lies above the threshold and can be identified through its narrow resonance in the $\bar{B}D$ invariant-mass spectrum. Studies of heavy-flavor hadron-associated production thus provide a powerful experimental avenue for the discovery of new hadronic states containing different heavy quarks.

A central experimental challenge in searches for doubly heavy tetraquarks at hadron colliders is the quantitative understanding of their prompt production and the associated backgrounds. In particular, the prompt production of heavy-meson pairs, such as BD, forms an irreducible background for tetraquark states decaying into two heavy mesons. A realistic description of such backgrounds is therefore essential for evaluating the experimental sensitivity and discovery potential for new states like T_{bc}.

From the perspective of production mechanisms, associated BD production proceeds primarily through single parton scattering (SPS) and multiparton scattering. The latter is dominated by double parton scattering (DPS), while contributions from higher-order multiparton interactions are expected to be suppressed. The relative importance of DPS is expected to increase with increasing proton-proton collision energy. Studies of associated BD production provide a sensitive probe of heavy-flavor production mechanisms, enable quantitative tests of SPS and DPS dynamics (see, e.g., ref. [16]), constrain heavy-quark correlations and fragmentation, and supply essential background information for searches for exotic states such as the T_{bc} tetraquark.

Previous theoretical studies have primarily focused on predicting the T_{bc} mass and width. However, a critical gap remains: a quantitative, data-driven assessment of the actual discovery potential at LHCb. This work aims to fill this gap by addressing the question: under what specific conditions – in terms of integrated luminosity, production cross section, and branching fraction – can a 5σ discovery of the T_{bc} be achieved amidst the formidable BD background? We provide a realistic evaluation of these conditions based on simulations calibrated to LHCb data.

Owing to the high heavy-flavor production rate in pp collisions, its excellent vertexing and tracking capability, efficient trigger, and precise control of detector-induced asymmetries, the LHCb experiment provides an ideal environment for searches for the T_{bc}.

The $T_{bc}(bc\bar{u}\bar{d})$ tetraquark with quantum numbers $J^P = 0^+$ are expected to decay strongly into $\bar{B}^0 D^0$, $B^- D^+$, and their charge-conjugate modes if the mass is above the meson-pair thresholds. This analysis investigates the experimental potential of the LHCb experiment to discover the T_{bc} through its production and decay into BD meson pairs. The study focuses on the decay chain

$$\begin{aligned} &T_{bc} \to B^- D^+, \\ &B^- \to J/\psi(\to \mu^+\mu^-)K^-, \\ &D^+ \to K^-\pi^+\pi^+, \end{aligned} \quad (2)$$

This provides a clean experimental signature for the discovery of the T_{bc} at LHCb.

Our approach maintains a close connection to experimental reality. The DPS background is calibrated using LHCb data, while the SPS contribution is evaluated with two different flavor-scheme calculations to account for theoretical uncertainties. Rather than relying on a single theoretical prediction, we treat $\sigma(T_{bc}) \times \mathcal{B}(T_{bc} \to B^- D^+)$ as a free parameter and scan over a well-motivated range, together with the T_{bc} mass, width, and effective DPS cross section σ_{eff}. After incorporating realistic reconstruction efficiencies, we translate the signal and background yields into the integrated luminosity required for a 5σ discovery. This work provides a quantitative benchmark for the T_{bc} search at LHCb and serves as a reference for future experimental studies in background-dominated environments.

II. METHOD

A. Background Simulations

In this analysis, both SPS and DPS processes are considered the dominant mechanisms contributing to the background in the $B^{\mp}D^{\pm}$ final state in the search for T_{bc}. The background samples for the two processes are generated separately, with the DPS sample reweighted to reproduce the differential distributions observed by LHCb. The following kinematic selection cuts are applied to both background samples to reflect the acceptance of the LHCb detector:

$$\begin{aligned} 2.0 < y_{B/D} < 4.5\,, \\ p_{\mathrm{T},B} < 40\ \mathrm{GeV}\,, \\ 1\ \mathrm{GeV} < p_{\mathrm{T},D} < 8\ \mathrm{GeV}\,. \end{aligned} \tag{3}$$

The SPS and DPS background samples are generated using `MadGraph5_aMC@NLO` (`MG5_aMC` hereafter) [17, 18], with parton showering and hadronization performed by `Pythia8.3` [19]. We consider proton-proton collisions at $\sqrt{s} = 13$ TeV. The charm- and bottom-quark masses are set to $m_c = 1.55$ GeV and $m_b = 4.7$ GeV, respectively. The `NNPDF2.3` parton distribution functions (PDFs) [20] are employed, with next-to-leading order (NLO) PDFs used for NLO simulations and leading order (LO) PDFs for LO simulations. Both the renormalization and factorization scales are chosen dynamically, with the central value given by $\mu_0 = H_T/2$, where H_T is the scalar sum of the transverse energies of the final-state particles. While the scale choice for the background process $pp \to b\bar{b}c\bar{c} + X$ is not uniquely defined, using $H_T/2$ is common practice in modern event generators, as it provides a natural estimate of the typical momentum transfer in such processes.

For simulating the SPS background, we consider two complementary approaches to generate samples. First, we study the process $pp \to b\bar{b}c\bar{c} + X$ in the 3-flavor number scheme (3FNS) at NLO in QCD, with matching to parton showers performed using the `MC@NLO` method [21]. We take the 3FNS calculation as the nominal prediction. The corresponding fiducial cross section, with fiducial cuts given in eq. (3), is found to be

$$\sigma^{\text{NLO SPS 3FNS}}_{B^{\mp}D^{\pm}} = 0.074^{+0.040}_{-0.034}\,\mu\mathrm{b}\,, \tag{4}$$

The uncertainty is dominated by variations in the renormalization and factorization scales. The fiducial cross section includes both B^-D^+ and B^+D^- final states. Together with the DPS contribution, this NLO SPS prediction defines the *baseline background scenario* used to assess the T_{bc} discovery potential.

Alternatively, as discussed in Ref. [22], the resummation of initial-state logarithms generated by gluon splitting into a charm-quark pair may be crucial for describing the LHCb $J/\psi + D$ measurement [23]. We therefore also generate the SPS sample at LO with charm- or anti-charm-gluon initial states in the 4-flavor number scheme (4FNS). This LO 4FNS calculation yields a fiducial cross section of

$$\sigma^{\text{LO SPS 4FNS}}_{B^{\mp}D^{\pm}} = 0.21^{+0.44}_{-0.15}\,\mu\mathrm{b}\,. \tag{5}$$

The dominant theoretical uncertainty arises from scale variations. As in the $J/\psi + D$ case [22], the 4FNS calculation significantly increases the SPS fiducial cross section relative to the 3FNS result. To obtain a conservative estimate of the T_{bc} discovery potential under a maximal-background assumption, we take the 1σ upper bound of the LO SPS 4FNS prediction, $\sigma^{\text{LO SPS 4FNS}}_{B^{\mp}D^{\pm},\text{max}} = 0.65\,\mu\mathrm{b}$, and combine it with the DPS contribution. This defines the *conservative maximal-background scenario*.

To simulate the DPS background, two NLO event samples for the processes $pp \to b\bar{b} + X$ and $pp \to c\bar{c} + X$ are generated independently. The DPS BD sample is obtained by randomly pairing events from the single-$B^{\mp}$ and single-$D^{\pm}$ samples. In the DPS approximation, the kinematic properties of the B and D mesons are largely governed by their respective single-particle distributions. However, the single-particle rapidity spectra predicted by `MG5_aMC` may differ from those observed in data. To reduce this model dependence, the DPS sample is reweighted on an event-by-event basis according to the rapidity difference $\Delta y = y_B - y_D$, using a reference Δy distribution constructed from the LHCb Run 2 measurements of the B- and D-meson single-particle $d\sigma/dy$ spectra [24, 25], as illustrated in Fig. 1.

The total fiducial cross section of the DPS process is

$$\sigma^{\text{DPS}}_{B^{\mp}D^{\pm}} = \frac{1}{2} \times \frac{\sigma_{B^{\mp}} \cdot \sigma_{D^{\pm}}}{\sigma_{\text{eff}}} = \left(\frac{15\ \mathrm{mb}}{\sigma_{\text{eff}}}\right) (2.4 \pm 0.3)\ \mu\mathrm{b}\,, \tag{6}$$

where $\sigma_{B^{\mp}} = (86.6 \pm 6.4)\,\mu\mathrm{b}$ [24] and $\sigma_{D^{\pm}} = (834 \pm 78)\,\mu\mathrm{b}$ [25], measured using the same fiducial cuts as in eq. (3). The factor of $1/2$ accounts for the fact that only the charge-neutral combinations B^-D^+ and B^+D^- are considered, since $\sigma_{B^{\mp}}$ and $\sigma_{D^{\pm}}$ include charge-conjugate contributions. The effective DPS cross section σ_{eff} is not precisely known but has been extracted from LHCb measurements of other heavy-flavor processes, such as $\Upsilon + D$ [26], $J/\psi + \Upsilon$ [27], and $J/\psi + D$ [22, 23], with typical values in the range 5-30 mb. In this analysis, we consider representative values $\sigma_{\text{eff}} = 5, 15$, and 30 mb.

Differential cross sections for associated $B^{\mp}D^{\pm}$ production via SPS, DPS, and their combination (SPS+DPS) are shown in Fig. \ref{fig:sps_dps_eff15}. The upper panels correspond to the NLO SPS prediction in the

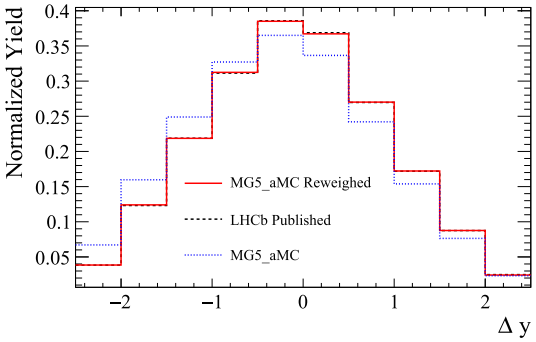

Fig. 1. (color online) Comparison of the rapidity difference Δy between the $B^{\mp}$ and $D^{\pm}$ mesons in the DPS background. The black dashed line represents the published LHCb Run 2 data, while the red solid and blue dotted lines correspond to the reweighted and unweighted DPS simulations, respectively. Results are shown for $\sigma_{\rm eff}$ = 15 mb.

3FNS, while the lower panels show the LO SPS prediction in the 4FNS. The shaded bands denote the combined statistical and systematic uncertainties. For both SPS and DPS, statistical uncertainties are estimated from the event samples. The DPS systematic uncertainty originates from the uncertainties on $\sigma_{B^{\mp}}$ and $\sigma_{D^{\pm}}$, whereas the SPS systematic uncertainty is dominated by variations of the renormalization and factorization scales in the perturbative calculations.

In the SPS mechanism, the azimuthal angle difference distribution, $\Delta\phi = |\phi(B) - \phi(D)|$, exhibits a prominent peak near π, indicating that $B^{\mp}$ and $D^{\pm}$ mesons are predominantly produced in a back-to-back configuration in the transverse plane. In contrast, the DPS mechanism yields a nearly uniform $\Delta\phi$ distribution, reflecting the absence of strong azimuthal correlations between the two mesons. Similarly, the rapidity gap Δy shows distinct features for the two mechanisms. SPS events produce an asymmetric Δy distribution, with the B meson typically more central in rapidity than the D meson, whereas DPS events result in a nearly symmetric distribution around $\Delta y = 0$, consistent with largely uncorrelated production of the two mesons. The invariant-mass distribution $M(B^{\mp}D^{\pm})$ further highlights these differences. SPS events, dominated by back-to-back configurations, lead to a relatively broad distribution with a pronounced high-mass tail, while DPS events produce a narrower peak, though occasional high-momentum combinations can generate a modest tail. Overall, these observables illustrate the distinct kinematic patterns of SPS and DPS and provide several handles for disentangling their respective contributions.

Within the LHCb kinematic acceptance, associated $B^{\mp}D^{\pm}$ production is dominated by the DPS mechanism when using the nominal NLO SPS prediction in the 3FNS, under which the SPS contribution is negligible. Only when adopting the conservative upper-bound LO SPS calculation in the 4FNS does the SPS contribution become comparable to DPS in certain kinematic regions.

These differential distributions, based on the kinematic cuts defined in eq. (3), will be used as the background for the T_{bc} search in subsequent analyses.

B. Generation of the T_{bc} Signal

In this analysis, the T_{bc} signal is generated assuming specific values for its mass $m(T_{bc})$, width $\Gamma(T_{bc})$, and production cross section $\sigma(T_{bc})$, motivated by theoretical expectations. Signal samples are produced for different mass and width hypotheses. The T_{bc} signal is modeled with a Breit–Wigner (BW) line shape to describe its natural width and is subsequently convolved with the detector response function to obtain the differential cross section.

The differential cross section for T_{bc} production can be written as

$$\frac{{\rm d}\sigma_{T_{bc}}}{{\rm d}m} = \sigma(T_{bc}) \int_{-\infty}^{+\infty} {\rm BW}(m') \cdot G(m - m', \sigma_{\rm res}) {\rm d}m' , \qquad (7)$$

where $\sigma(T_{bc}) \equiv \sigma(pp \to T_{bc} + X) + \sigma(pp \to \overline{T}_{bc} + X)$ denotes the total production cross section for the T_{bc} and $\overline{T}_{bc}$ states within the LHCb acceptance $(2 < \eta(T_{bc}) < 4.5)$[1)], and $m \equiv M(B^{\mp}D^{\pm})$ denotes the invariant mass of the reconstructed $B^{\mp}D^{\pm}$ pair. The nonrelativistic BW distribution is given by

$${\rm BW}(m') = \frac{1}{2\pi} \frac{\Gamma(T_{bc})}{(m' - m(T_{bc}))^2 + (\Gamma(T_{bc})/2)^2} . \qquad (8)$$

The detector response function G is modeled as a Gaussian distribution:

$$G(m - m', \sigma_{\rm res}) = \frac{1}{\sqrt{2\pi}\sigma_{\rm res}} \exp\left[- \frac{(m - m')^2}{2\sigma_{\rm res}^2} \right] , \qquad (9)$$

motivated by LHCb measurements of similar decay modes, such as $B_c^+ \to J/\psi D_s^+$ and $B_c^+ \to B_s^0(\to D_s^- \pi^+)\pi^+$ [29], for which the mass resolution is found to be in the range 4-7 MeV. Given that the $T_{bc} \to B^- D^+$ decay chain, eq. (2), involves multiple tracks and allows for intermediate mass constraints, we adopt a mass resolution of $\sigma_{\rm res}$ = 6 MeV in the simulation.

In this study, we consider two representative mass hy-

1) To obtain the inclusive cross section, or the inclusive limit on $\sigma(T_{bc}) \times \mathcal{B}$, over the full phase space (i.e., without fiducial cuts), the fiducial results should be divided by the LHCb acceptance. The acceptance is estimated to be 22–24% based on simulations of Ξ_{bc} and B_c production and is assumed to be similar for T_{bc} production.

potheses for the T_{bc}, $m(T_{bc}) = 7167$ MeV and $m(T_{bc}) = 7229$ MeV, motivated by theoretical predictions for exotic hadron states with quantum numbers $J^P = 0^+$ [5, 13]. These values correspond to possible T_{bc} configurations and span a reasonable range consistent with current theoretical expectations for heavy tetraquarks. For these mass hypotheses, we consider several representative values of the width and production cross section. The width values $\Gamma(T_{bc}) = 0.5$, 5 MeV are used for $m(T_{bc}) = 7167$ MeV, while $\Gamma(T_{bc}) = 10$, 40 MeV are adopted for $m(T_{bc}) = 7229$ MeV. These choices are motivated by comparisons with similar exotic hadrons: the narrow width of the T_{cc}^+ ($\Gamma(T_{cc}^+) \sim 0.4$ MeV) [2], and the broader widths of states such as $Z_c(3900)$ and $Z_b(10610)$, which have widths of order 10-30 MeV [30, 31].

The theoretical prediction for the T_{bc} production cross section is highly uncertain, with different approaches yielding results that can differ by two orders of magnitude, ranging from a very conservative value of 0.3 nb [32] to an optimistic estimate of 103 nb [33]. In addition to the two spanning a wide range, we also consider an intermediate estimate using

$$\sigma(T_{bc}) \approx \sigma(T_{cc}^+) \times \frac{\sigma(\Xi_{bc})}{\sigma(\Xi_{cc})} \approx 45 \times 0.4 \approx 18\ \text{nb}, \tag{10}$$

where $\sigma(T_{cc}^+) = 45 \pm 20$ nb is the prompt production cross section of the T_{cc}^+ tetraquark at LHCb within the typical acceptance ($2 < p_T/\text{GeV} < 20$, $2.0 < y < 4.5$) [34], and $\sigma(\Xi_{bc})/\sigma(\Xi_{cc}) \approx 0.4$ is adopted from theoretical calculations of doubly heavy baryon production at LHC energies [35]. In summary, all three representative values (optimistic: 103 nb, intermediate: 18 nb, conservative: 0.3 nb) are considered in this study.

Based on these assumptions, we simulate the T_{bc} signal and evaluate the discovery potential across different parameter combinations. Since the T_{bc} resonance is narrow and the background is largely smooth in the $B^{\mp}D^{\pm}$ invariant mass spectrum, signal-background interference is expected to be small. In particular, the interference effect decreases as the signal width $\Gamma(T_{bc})$ decreases and can be safely neglected for the narrowest width considered ($\Gamma(T_{bc}) = 0.5$ MeV). Therefore, we neglect signal-background interference in our study.

C. Signal and Background Yields

In this analysis, once the cross-section distributions for the signal and background have been constructed, the numbers of signal and background events are estimated based on the decay chain in Eq. (2). The event yields for both signal and background are then computed using the standard event-counting formula:

$$N = \sigma \times \mathcal{L}_{\text{int}} \times \mathcal{B} \times \varepsilon, \tag{11}$$

where

- σ denotes the production cross section. For the signal, $\sigma = \sigma(T_{bc})$, whereas for the background it is the sum of the SPS and DPS contributions: $\sigma = \sigma^{\text{DPS}}_{B^{\mp}D^{\pm}} + \sigma^{\text{SPS}}_{B^{\mp}D^{\pm}}$. In this study, we neglect the dependence of σ on the pp center-of-mass energy between 13 TeV and 14 TeV.

- $\mathcal{L}_{\text{int}}$ is the integrated luminosity. LHCb has already collected approximately 6 fb^{-1} of pp collision data in Run 2 at $\sqrt{s} = 13$ TeV. The Run 1 dataset is not included in this study, as its relatively small integrated luminosity and lower center-of-mass energies (7 and 8 TeV) make a negligible contribution to the overall sensitivity. By the end of Run 4, the total integrated luminosity from Runs 2, 3, and 4 is expected to reach ~ 50 fb^{-1}, and by the end of Run 5 it is expected to reach ~ 300 fb^{-1}. Therefore, in this study we scan $\mathcal{L}_{\text{int}}$ over the range 5-300 fb^{-1}.

- $\mathcal{B}$ denotes the branching fraction. The relevant values are $\mathcal{B}(B^{\pm} \to J/\psi K^{\pm}) = (1.020 \pm 0.019) \times 10^{-3}$, $\mathcal{B}(D^{\pm} \to K^{\mp}\pi^{\pm}\pi^{\pm}) = (9.38 \pm 0.16) \times 10^{-2}$, and $\mathcal{B}(J/\psi \to \mu^+\mu^-) = (5.961 \pm 0.033) \times 10^{-2}$ [36]. For the signal decay $T_{bc} \to B^-D^+$, we adopt a default branching fraction $\mathcal{B}(T_{bc} \to B^-D^+) = 0.5$. This choice is motivated by the expectation that the $J^P = 0^+$ T_{bc} state decays predominantly into the two open-heavy-flavor channels, $\bar{B}^0D^0$ and B^-D^+, with comparable rates. In the absence of detailed theoretical calculations, this symmetric assignment serves as a reasonable reference point, and the associated uncertainty is effectively accounted for by the scan over $\sigma(T_{bc}) \times \mathcal{B}$ presented in Tables 3 and 4.

- ε denotes the overall event reconstruction and selection efficiency, including contributions from the detector geometric acceptance, track reconstruction, trigger, particle identification, and offline selection. For the decay $T_{bc} \to B^-D^+$, the efficiency is given by the product $\varepsilon_B \times \varepsilon_D$, with the D-meson trigger efficiency excluded, since the BD candidates are triggered by the B meson. The total efficiency is estimated using measurements of related decays [24, 25], yielding $\varepsilon_{BD} = (0.6 \pm 0.3)\%$; the 50% relative uncertainty is a conservative estimate that accounts for potential correlations between the two efficiency factors and for variations across the full kinematic range and different data-taking conditions.

Figure 3 shows an example of the invariant-mass spectrum of the reconstructed $B^{\mp}D^{\pm}$ pairs at an integrated luminosity of 50 fb^{-1}, assuming a T_{bc} production cross section $\sigma(T_{bc}) = 103$ nb and an effective DPS cross section $\sigma_{\text{eff}} = 15$ mb. In this case, the T_{bc} signal appears as a distinct resonance peak at the expected mass.

D. Discovery Potential

After obtaining the signal and background yields, N_{Sig}

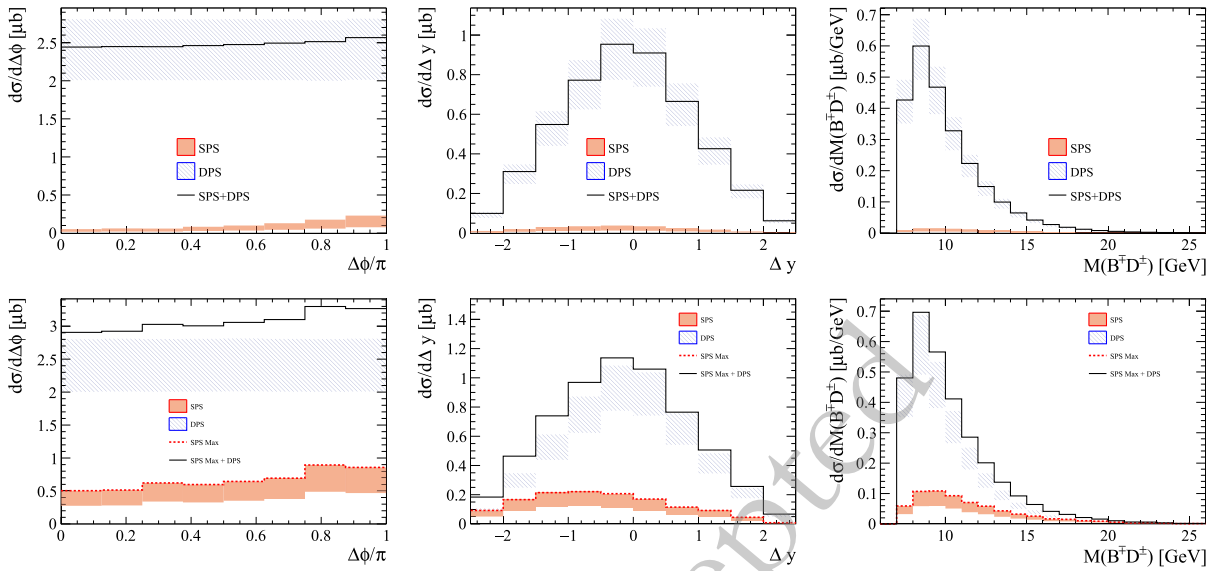

Fig. 2. (color online) Differential cross sections for associated $B^{\mp}D^{\pm}$ production via SPS and DPS. Left: $\Delta\phi$ distribution; middle: Δy distribution; right: invariant-mass $M(B^{\mp}D^{\pm})$ distribution, shown for $\sigma_{\rm eff}$ = 15 mb. The upper (lower) panels show the SPS prediction at NLO in the 3FNS (LO in the 4FNS). The SPS contribution is displayed as a red shaded band, with uncertainties dominated by renormalization- and factorization-scale variations, while the DPS contribution is displayed as a blue hatched band. In the upper panels, the black solid line denotes the combined SPS+DPS central prediction, which defines the baseline background scenario. In the lower panels, the red dashed line indicates the maximal SPS contribution, taken from the upper bound of the LO 4FNS prediction, while the black solid line shows the corresponding SPS (max)+DPS prediction, which defines the conservative maximal background scenario.

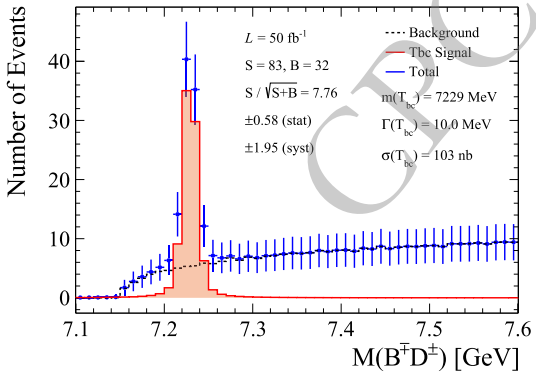

Fig. 3. (color online) Combined distribution of the T_{bc} signal and background in the BD invariant-mass spectrum, assuming an effective DPS cross section $\sigma_{\rm eff}$ = 15 mb, $m(T_{bc})$ = 7229 MeV, and $\Gamma(T_{bc})$ = 10 MeV. The black curve represents the $B^{\mp}D^{\pm}$ background, the red curve the T_{bc} signal, and the blue curve their sum.

and $N_{\rm Bkg}$, under different parameter assumptions, the significance of the T_{bc} signal is estimated using the standard formula:

$$Z = \frac{N_{\rm Sig}}{\sqrt{N_{\rm Sig} + N_{\rm Bkg}}}, \tag{12}$$

where $N_{\rm Sig}$ and $N_{\rm Bkg}$ denote the numbers of signal and background events within a $\pm 3\sigma_{\rm eff\,res}$ mass window, as evaluated using Eq. (11). The effective mass resolution is defined as

$$\sigma_{\rm eff\,res} = \sqrt{\left(\frac{\Gamma(T_{bc})}{2.35}\right)^2 + \sigma_{\rm res}^2}, \tag{13}$$

The mass window is centered on the signal peak in the $B^{\mp}D^{\pm}$ invariant-mass spectrum.

In this study, we evaluate the discovery potential of T_{bc} by scanning the significance Z as a function of the integrated luminosity $\mathcal{L}_{\rm int}$ for different T_{bc} mass and width hypotheses, as well as different values of the effective DPS cross section $\sigma_{\rm eff}$ that contribute to the background. This scan allows us to determine the minimum integrated luminosity required for a 5σ discovery of T_{bc} under these assumptions.

In addition, we scan over $\sigma(T_{bc})\times\mathcal{B}(T_{bc}\to B^-D^+)$ to evaluate how different assumed signal strengths affect the discovery significance. By calculating Z for various integrated luminosities, we determine the minimum observable value of $\sigma(T_{bc})\times\mathcal{B}(T_{bc}\to B^-D^+)$ corresponding to a 5σ threshold, providing a quantitative assessment of the T_{bc} discovery potential under different experimental conditions.

E. Systematic Uncertainties

In this study, several sources of systematic uncertainty affect the estimate of the significance Z. The

branching fractions $\mathcal{B}(B^{\pm} \to J/\psi K^{\pm})$, $\mathcal{B}(J/\psi \to \mu^{+}\mu^{-})$, and $\mathcal{B}(D^{+} \to K^{-}\pi^{+}\pi^{+})$ are taken from ref. [36], with relative uncertainties of 1.9%, 0.6%, and 1.7%, respectively. The detector efficiency, $\varepsilon = (0.6 \pm 0.3)\%$, corresponds to a 50% relative uncertainty. These uncertainties are fully correlated between signal and background because both yields depend on the same inputs.

An additional uncertainty affects only the background yield and arises from uncertainties in the measured $B^{\mp}$ and $D^{\pm}$ production cross sections. Propagating the uncertainties on $\sigma_{B^{\mp}}$ and $\sigma_{D^{\pm}}$ yields an approximate 10% relative uncertainty in the DPS background cross section. The normalization of the DPS cross section is also subject to significant uncertainty due to σ_{eff}, which is included in our evaluation. The SPS background uncertainty is evaluated using the baseline and conservative scenarios described in Section II A.

The total systematic uncertainty on the significance Z is computed by propagating these uncertainties, accounting for the correlation structure outlined above. Among the considered sources, the detector-efficiency uncertainty dominates. This procedure is applied to each parameter scenario and is reflected in all results presented in Section III.

III. RESULTS

A. Minimum Integrated Luminosity for a 5σ Discovery at LHCb

Figure 4 shows the statistical significance Z of the T_{bc} signal in the BD invariant-mass spectrum as a function of integrated luminosity $\mathcal{L}_{\text{int}}$, for different values of the effective DPS cross section σ_{eff} and for various assumptions on the T_{bc} mass and width. The top, middle, and bottom panels correspond to production cross sections of $\sigma(T_{bc}) = 103$ nb, 18 nb, and 0.3 nb, respectively. We assume a baseline background scenario and take the branching fraction to be $\mathcal{B}(T_{bc} \to B^{-}D^{+}) = 0.5$. The values of σ_{eff} are set to 5, 15, and 30 mb, from left to right.

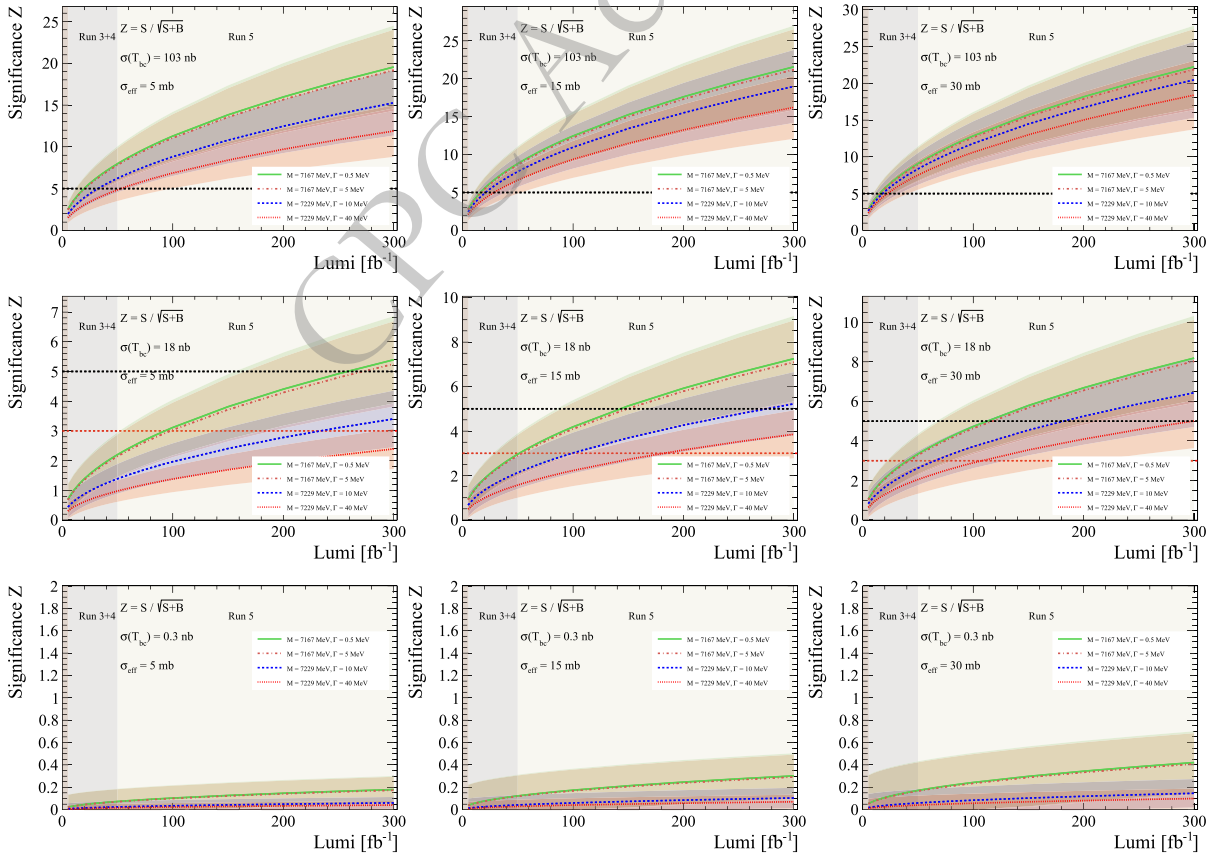

Fig. 4. (color online) Shown is the statistical significance Z of the T_{bc} signal in the BD invariant-mass spectrum as a function of the integrated luminosity $\mathcal{L}_{\text{int}}$, for different T_{bc} mass and width assumptions and for various values of the effective DPS cross section σ_{eff}. The top, middle, and bottom panels correspond to production cross sections $\sigma(T_{bc}) = 103$ nb, 18 nb, and 0.3 nb, respectively. A baseline background scenario (DPS + NLO SPS in the 3FNS) and a branching fraction $\mathcal{B}(T_{bc} \to B^{-}D^{+}) = 0.5$ are assumed. The left, middle, and right panels correspond to $\sigma_{\text{eff}} = 5$ mb, 15 mb, and 30 mb, respectively. Different colors denote different T_{bc} mass and width assumptions: $M = 7167$ MeV with $\Gamma = 0.5$, 5 MeV, and $M = 7229$ MeV with $\Gamma = 10$, 40 MeV, where $M \equiv m(T_{bc})$ and $\Gamma \equiv \Gamma(T_{bc})$. The dashed line indicates the 5σ discovery threshold.

As $\sigma_{\rm eff}$ increases, the DPS background cross section decreases, thereby enhancing the discovery potential for T_{bc}.

For the optimistic estimate of $\sigma(T_{bc}) = 103$ nb (top panels), Fig. 5 and Table 1 show the minimum integrated luminosity required for a 5σ discovery. For most parameter sets, this is achievable with 50 fb^{-1} (Run 2 + Run 3 + Run 4). A comparison between baseline and conservative background scenarios indicates that this requirement is robust against SPS modeling uncertainties. For the intermediate estimate of $\sigma(T_{bc}) = 18$ nb, the discovery potential is reduced relative to the optimistic case. Table 2 shows the minimum integrated luminosity required for 3σ evidence and 5σ discovery. At 300 fb^{-1}, corresponding to the full LHCb dataset up to Run 5, the significance exceeds 3σ for most parameter sets, and only the most favorable scenarios reach 5σ. In the most pessimistic scenario with $\sigma(T_{bc}) = 0.3$ nb, the statistical significance remains well below 3σ for all parameter sets considered, even with 300 fb^{-1}. Under this pessimistic assumption, no significant signal is expected.

B. Minimum Cross Section times Branching Fraction for a 5σ Discovery of T_{bc} at LHCb

Tables 3 and 4 show the minimum observable values of the product $\sigma(T_{bc}) \times \mathcal{B}(T_{bc} \to B^- D^+)$ required to achieve a 5σ discovery of T_{bc} for different integrated-luminosity scenarios. Table 3 corresponds to $\mathcal{L}_{\rm int} = 50$ fb^{-1}, combining data from Runs 2–4, while Table 4 corresponds to $\mathcal{L}_{\rm int} = 300$ fb^{-1}, including data from Runs 2–5. Increasing the integrated luminosity from 50 fb^{-1} to 300 fb^{-1} substantially lowers the minimum observable

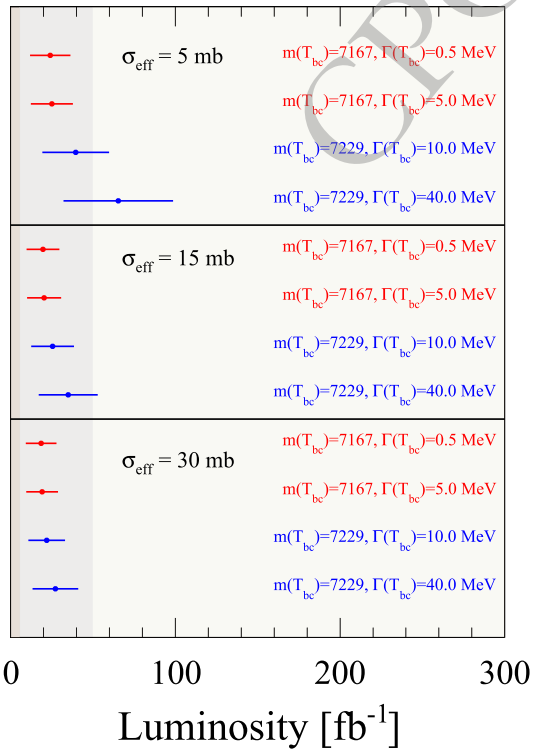

Fig. 5. (color online) Discovery significance for T_{bc} as a function of integrated luminosity for different T_{bc} mass and width parameters, assuming the baseline background scenario with $\sigma(T_{bc}) = 103$ nb and $\mathcal{B}(T_{bc} \to B^- D^+) = 0.5$.

Table 1. The integrated luminosity required for a 5σ discovery is evaluated under different T_{bc} parameter assumptions, assuming $\sigma(T_{bc}) = 103$ nb and $\mathcal{B}(T_{bc} \to B^- D^+) = 0.5$. Both the baseline and a conservative, maximal-background scenario are considered. The quoted uncertainties include both statistical and systematic contributions.

DPS $\sigma_{\rm eff}$ [mb]	m(T_{bc}), $\Gamma(T_{bc})$ [MeV]	$\mathcal{L}_{\rm int}$ [fb^{-1}] (NLO SPS 3FNS)	$\mathcal{L}_{\rm int}$ [fb^{-1}] (LO SPS 4FNS, max)
5	7167, 0.5	24 ± 12	25 ± 13
	7167, 5.0	25 ± 13	26 ± 13
	7229, 10	40 ± 20	40 ± 21
	7229, 40	66 ± 33	68 ± 34
15	7167, 0.5	20 ± 10	20 ± 10
	7167, 5.0	21 ± 10	21 ± 10
	7229, 10	26 ± 13	26 ± 13
	7229, 40	35 ± 18	37 ± 19
30	7167, 0.5	19 ± 9	19 ± 10
	7167, 5.0	19 ± 10	20 ± 10
	7229, 10	22 ± 11	23 ± 11
	7229, 40	27 ± 14	29 ± 15

Table 2. Integrated luminosities required for 3σ evidence and 5σ discovery of the T_{bc} state under different baseline background assumptions. The calculation assumes $\sigma(T_{bc}) = 18$ nb and $\mathcal{B}(T_{bc} \to B^- D^+) = 0.5$. Entries marked with "–" indicate that the required luminosity exceeds 300 fb^{-1}. The quoted uncertainties include both statistical and systematic components.

DPS $\sigma_{\rm eff}$ [mb]	m(T_{bc}), $\Gamma(T_{bc})$ [MeV]	$\mathcal{L}_{\rm int}$ [fb^{-1}] (3 σ)	$\mathcal{L}_{\rm int}$ [fb^{-1}] (5 σ)
5	7167, 0.5	117 ± 65	318 ± 162
	7167, 5.0	123 ± 68	335 ± 170
	7229, 10	290 ± 152	–
	7229, 40	585 ± 298	–
15	7167, 0.5	64 ± 37	175 ± 90
	7167, 5.0	68 ± 39	183 ± 94
	7229, 10	124 ± 69	339 ± 172
	7229, 40	226 ± 120	–
30	7167, 0.5	50 ± 29	137 ± 70
	7167, 5.0	52 ± 30	143 ± 73
	7229, 10	82 ± 47	223 ± 114
	7229, 40	134 ± 74	368 ± 186

Table 3. Minimum observable value of $\sigma(T_{bc})\times\mathcal{B}(T_{bc}\to B^-D^+)$ required to achieve a 5σ discovery of T_{bc} at $\mathcal{L}_{\rm int}=50\,{\rm fb}^{-1}$ (Runs 2–4), for different T_{bc} parameter assumptions, shown for both the baseline and conservative, maximal-background scenarios. The quoted uncertainties include both statistical and systematic contributions.

DPS $\sigma_{\rm eff}$ [mb]	m(T_{bc}), $\Gamma(T_{bc})$ [MeV]	$\sigma(T_{bc})\times\mathcal{B}$ [nb] (NLO SPS 3FNS)	$\sigma(T_{bc})\times\mathcal{B}$ [nb] (LO SPS 4FNS, max)
5	7167, 0.5	30 ± 11	30 ± 11
	7167, 5.0	31 ± 11	31 ± 12
	7229, 10	43 ± 15	44 ± 15
	7229, 40	60 ± 19	60 ± 19
15	7167, 0.5	23 ± 10	23 ± 10
	7167, 5.0	24 ± 10	24 ± 10
	7229, 10	31 ± 12	31 ± 12
	7229, 40	40 ± 14	41 ± 14
30	7167, 0.5	21 ± 9	21 ± 9
	7167, 5.0	21 ± 10	22 ± 10
	7229, 10	26 ± 11	27 ± 11
	7229, 40	32 ± 12	34 ± 13

Table 4. Minimum observable $\sigma(T_{bc})\times\mathcal{B}(T_{bc}\to B^-D^+)$ required for a 5σ discovery of T_{bc} at $\mathcal{L}_{\rm int}=300\,{\rm fb}^{-1}$ (combined Run 2, Run 3, and Run 4), under various T_{bc} parameter assumptions, is shown for both the baseline and conservative maximal-background scenarios. The quoted uncertainties include both statistical and systematic contributions.

DPS $\sigma_{\rm eff}$ [mb]	m(T_{bc}), $\Gamma(T_{bc})$ [MeV]	$\sigma(T_{bc})\times\mathcal{B}$ [nb] (NLO SPS 3FNS)	$\sigma(T_{bc})\times\mathcal{B}$ [nb] (LO SPS 4FNS, max)
5	7167, 0.5	9 ± 3	10 ± 3
	7167, 5.0	10 ± 3	10 ± 3
	7229, 10	15 ± 4	15 ± 4
	7229, 40	21 ± 6	22 ± 6
15	7167, 0.5	6 ± 2	6 ± 2
	7167, 5.0	6 ± 2	7 ± 2
	7229, 10	10 ± 3	10 ± 3
	7229, 40	13 ± 4	14 ± 4
30	7167, 0.5	5 ± 2	5 ± 2
	7167, 5.0	5 ± 2	6 ± 2
	7229, 10	7 ± 2	8 ± 3
	7229, 40	10 ± 3	11 ± 3

$\sigma(T_{bc})\times\mathcal{B}(T_{bc}\to B^-D^+)$, thereby enhancing statistical sensitivity. In particular, the minimum observable value is reduced by a factor of three or more, depending on the assumed T_{bc} parameters and background scenarios.

Assuming $\sigma(T_{bc})\times\mathcal{B}(T_{bc}\to B^-D^+)$ lies in the range 20–60 nb, a 5σ observation of T_{bc} could be achieved by the end of Run 4. Smaller values, in the range 5–25 nb, would require the full Run 5 dataset. These results emphasize that both the integrated luminosity and the production cross section times branching fraction are key determinants of the discovery potential.

IV. SUMMARY

In this study, we investigate the discovery potential of the T_{bc} state at the LHCb experiment using a phenomenological approach. The background is modeled with `MG5_aMC` and `Pythia8.3` generators, with simulations tuned to published LHCb measurements. We scan the parameter space of the T_{bc} mass (7167–7229 MeV), width (0.5–40 MeV), production cross section ($\sigma(T_{bc})=0.3, 18, 103$ nb), and effective DPS cross section ($\sigma_{\rm eff}=5, 15, 30$ mb) to determine the integrated luminosity required for a 5σ discovery.

Our results indicate that, for the optimistic production cross section of $\sigma(T_{bc})=103$ nb and a branching fraction of $\mathcal{B}(T_{bc}\to B^-D^+)=0.5$, a 5σ discovery is expected by the end of Run 4, except in the case of a heavy, broad T_{bc} state ($m_{T_{bc}}=7229$ MeV, $\Gamma(T_{bc})=40$ MeV) with a large DPS background ($\sigma_{\rm eff}=5$ mb), for which the significance is nevertheless still sizable. For the intermediate estimate of $\sigma(T_{bc})=18$ nb, most parameter choices yield a 3σ evidence with the full Run 5 dataset, while only the most favorable scenarios reach 5σ. In the most conservative scenario of $\sigma(T_{bc})=0.5$ nb, no signal would be observable even with 300 fb^{-1}.

We also evaluated the minimum observable $\sigma(T_{bc})\times\mathcal{B}(T_{bc}\to B^-D^+)$ required for a 5σ discovery under different integrated luminosity scenarios. With 50 fb^{-1} of data (Run 2 to Run 4), a discovery is expected if $\sigma(T_{bc})\times\mathcal{B}(T_{bc}\to B^-D^+)$ lies between 20 nb and 60 nb. For smaller cross sections in the range 5 nb to 25 nb, the full Run 5 dataset (300 fb^{-1}) is needed.

In conclusion, this work provides a quantitative, data-driven assessment of the T_{bc} discovery potential at LHCb, addressing the challenge of background modeling for prompt $\bar{B}D$ production. A systematic search for the T_{bc} at LHCb is feasible, with promising prospects for evidence (3σ) and potential discovery (5σ), depending on the integrated luminosity and T_{bc} production cross section. Even in the absence of a signal, these results provide valuable theoretical input by setting upper limits on $\sigma(T_{bc})\times\mathcal{B}(T_{bc}\to B^-D^+)$, thereby offering experimental constraints to guide hadron models. Together, these findings establish a foundation for further exploration of exotic hadrons at LHCb.

ACKNOWLEDGMENTS

We are grateful to Xiaojie Jiang, Ivan Polyakov and

Xuhao Yuan for useful discussions. Views and opinions expressed are however, those of the authors only and do not necessarily reflect those of the European Union or the European Research Council Executive Agency. Neither the European Union nor the granting authority can be held responsible for them.

References

[1] Choi, S. K., *et al*., Phys. Rev. Lett. **91**, 262001 (2003)
[2] Aaij, R., *et al*., Nature Phys. **18**, 751 (2022)
[3] Aaij, R., *et al*., Phys. Rev. Lett. **121**, 162002 (2018)
[4] Deng, C. and Zhu, S.-L., Phys. Rev. D **105**, 054015 (2022)
[5] Cheng, J.-B., Li, S.-Y., Liu, Y.-R., Si, Z.-G., and Yao, T., Chin. Phys. C **45**, 043102 (2021)
[6] Chen, W., Steele, T. G., and Zhu, S.-L., Phys. Rev. D **89**, 054037 (2014)
[7] Karliner, M. and Rosner, J. L., Phys. Rev. Lett. **119**, 202001 (2017)
[8] Caramés, T. F., Vijande, J., and Valcarce, A., Phys. Rev. D **99**, 014006 (2019)
[9] Radhakrishnan, A., Padmanath, M., and Mathur, N., Phys. Rev. D **110**, 034506 (2024)
[10] Meinel, S., Pflaumer, M., and Wagner, M., Phys. Rev. D **106**, 034507 (2022)
[11] Wu, W.-L., Ma, Y., Chen, Y.-K., Meng, L., and Zhu, S.-L., Phys. Rev. D **110**, 094041 (2024)
[12] Ebert, D., Faustov, R. N., Galkin, V. O., and Lucha, W., Phys. Rev. D **76**, 114015 (2007)
[13] Eichten, E. J. and Quigg, C., Phys. Rev. Lett. **119**, 202002 (2017)
[14] Song, Y. and Jia, D., Commun. Theor. Phys. **75**, 055201 (2023)
[15] Xing, Y. and Zhu, R., Phys. Rev. D **98**, 053005 (2018)
[16] Maciuła, R. and Szczurek, A., Phys. Rev. D **97**, 094010 (2018)
[17] Alwall, J., *et al*., JHEP **07**, 079 (2014)
[18] Frederix, R. *et al*., JHEP **07** (2018) 185, [Erratum: JHEP 11, 085 (2021)].
[19] Bierlich, C., *et al*., SciPost Phys. Codeb. **2022**, 8 (2022)
[20] Ball, R. D., *et al*., Nucl. Phys. B **867**, 244 (2013)
[21] Frixione, S. and Webber, B. R., JHEP **06**, 029 (2002)
[22] Shao, H.-S., Phys. Rev. D **102**, 034023 (2020)
[23] Aaij, R. *et al*., JHEP **06** (2012) 141, [Addendum: JHEP 03, 108 (2014)].
[24] Aaij, R., *et al*., JHEP **12**, 026 (2017)
[25] Aaij, R., *et al*., JHEP **03**, 159 (2016)
[26] Aaij, R., *et al*., JHEP **07**, 052 (2016)
[27] Aaij, R., *et al*., JHEP **08**, 093 (2023)
[28] To obtain the inclusive cross section, or the inclusive limit on $\sigma(T_{bc})\times\mathcal{B}$, over the full phase space (i.e., without fiducial cuts), the fiducial results should be divided by the LHCb acceptance. The acceptance is estimated to be 22–24% based on simulations of Ξ_{bc} and B_c production and is assumed to be similar for T_{bc} production.
[29] Aaij, R., *et al*., JHEP **07**, 123 (2020)
[30] Ablikim, M., *et al*., Phys. Rev. Lett. **110**, 252001 (2013)
[31] Garmash, A., *et al*., Phys. Rev. Lett. **116**, 212001 (2016)
[32] Chen, Y.-q. and Wu, S.-z., Phys. Lett. B **705**, 93 (2011)
[33] Ali, A., Qin, Q., and Wang, W., Phys. Lett. B **785**, 605 (2018)
[34] Ali, A., Ahmed, I., and Aslam, M. J., Phys. Lett. B **855**, 138779 (2024)
[35] Zhang, J.-W., Wu, X.-G., Zhong, T., Yu, Y., and Fang, Z.-Y., Phys. Rev. D **83**, 034026 (2011)
[36] Navas, S., *et al*., Phys. Rev. D **110**, 030001 (2024)